MICRORELAY PACKAGING TECHNOLOGY USING FLIP-CHIP ASSEMBLY

David C. Miller, Wenge Zhang, and Victor M. Bright

NSF Center for Advanced Manufacturing and Packaging of Microwave, Optical, and Digital Electronics
Department of Mechanical Engineering, University of Colorado, Boulder, CO 80309-0427
http://mems.colorado.edu

ABSTRACT

Using flip-chip assembly, micromachined connectors can be used to create a high density, actuatable electronics packaging technology. Internal residual stress is used to press bimorph beam connectors upwards against a device chip. Deformation can be increased by introducing stress through a heat treating process. The effects of heat treatment are more prominent on larger devices and are long lasting in nature. The connectors' actuation behavior is described, including appropriate mathematical models. The electrostatically actuated beams will disconnect when driven by a 53 volt signal and will reconnect when voltage falls below 43 volts. When switching signals, reconnection occurs in as little as 5.8 μs, disconnection occurs in as little as 4.0 μs. A microconnector's current carrying capability can be as high as 285.3 mA and its maximum power dissipation as high as 1.47 W.

INTRODUCTION

Ball Grid Array and subsequent families comprise the current state of the art in high-density electronics packaging. By using microdevices in the place of solder, one creates a new family of packaging technology, Figure 1. Our design consists of cantilever microconnectors that can be used in a relay-like manner. Previous research includes early microrelay research [1,2], more recent electrostatic cantilever devices [3,4] and wafer probe devices, a similar application [5,6]. Our microconnector design is a combination of both the microrelay and wafer probe concepts. The use of MEMS in electronics packaging offers unique advantages at the chip to chip-carrier level. Lead count (input/ output) to device chips* has become a principle factor in design, limiting the amount of electronics that may be placed on a circuit board. The precision provided through micromachining fabrication can to create compact connection sites, greatly improving lead count. Use of microdevices in packaging also allows the possibility of a dynamic (switchable) connection. This permits redundant (backup) and alternative systems to be entirely connected or disconnected as need be. In this way, systems remain electrically isolated, preventing damage, when not in use. The dynamic connection also allows logic functions to be integrated into the connections between chips in multi-chip-modules and three-dimensional (stacked) devices. Logic functions can be realized when the connector is made to function as a mechanical transistor.

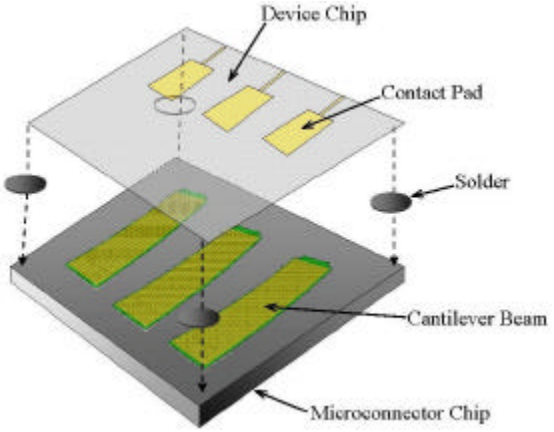

Figure 1: High Density Microconnector Array Fabricated Using Flip-Chip Assembly.

DEVICES AND DEVICE ASSEMBLY

The microconnector consists of a bimorph beam, composed of silicon and gold, Figure 2. To demonstrate the microconnector concept, the MUMPs foundry process [7], was used to fabricate prototypes. Once released, residual stress within the beam will cause it to curl upwards, away from the substrate, Figure 3. The stress ensures that the connector will normally be in contact with a device chip located above it. Beneath the beam is a polysilicon electrode, which can be used to electrostatically actuate the connector. Electrostatic attraction pulls the beam down towards the electrode, breaking the connection with the device chip above. Because the connector is actuatable, it may be utilized in the same manner as a conventional transistor. The "pins" are labeled appropriately, Figure 2.

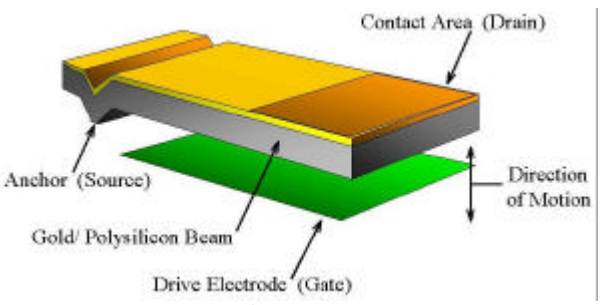

Figure 2: Parts of a Microconnector Device.

* The term "device chip" refers to any electronics chip that is to be packaged, whether it is an integrated circuit or another MEMS chip.

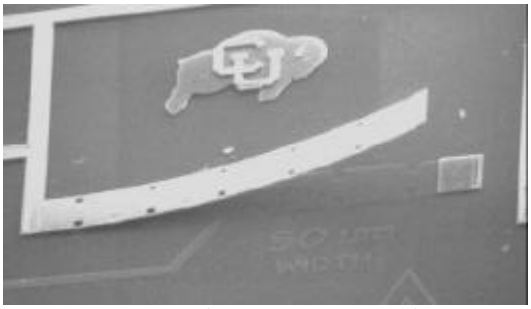

Figure 3: Micrograph of Microconnector. Deflection Occurs Naturally Due to Residual Stress Within the Beam.

To characterize the microconnector design, 3 x 3 arrays of connectors were flip-chip assembled to a test "device" chip, Figure 4. The device chips, composed of borosilicate glass, feature gold traces that were patterned using photolithography. The thermal coefficient of expansion of the glass chips is matched to that of silicon. The glass chip is also transparent, allowing for post-assembly inspection of the connectors. Pads and traces on the chip allow gold to gold metallic connection to be made between connectors and the device chip.

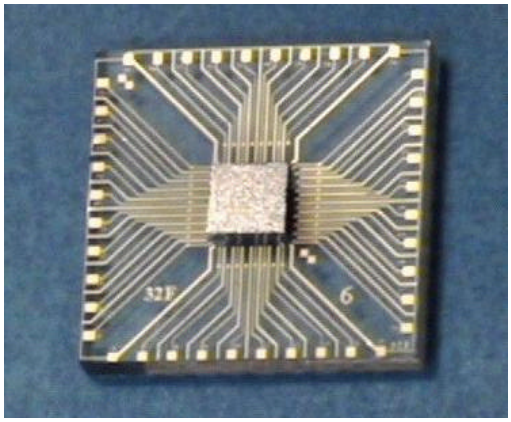

Figure 4: A Microconnector Chip is Assembled Face-Down (Center) on top of the Glass "Device" Chip.

The flip chip assembly process may be performed as follows: First, one adds solder to the device chip. Sn/Pb (63/37) solder balls can be manually placed and reflowed onto the chip. Other possible solder placement methods include electroplating or evaporation. Deposited solder, such as indium, can be patterned using photolithography, followed by a lift-off process. Next, the microconnectors are released using a HF soak, followed by supercritical CO_2 drying [8]. The microconnector and device chips are then placed on a flip-chip bonding machine and optically aligned. The face to face alignment should be reasonably precise. If used carefully, our machine is accurate within 10 μm. Flip-chip assembly occurs when the chips are pressed together on a heated stage. Immediately following assembly, the solder is reflowed to improve electrical connectivity. Reflow is performed in a formic acid environment, effectively providing a gaseous flux [9]. The gap between the microconnector and device chips was nominally 12 μm. For the purposes of testing, our devices were packaged using a DIP package.

Several aspects of our prototype assembly process might be performed differently if manufacture were to occur in industry. During the assembly of prototypes, the hot stage forces the microconnectors to flatten out, preventing damage. In an actual application, the microconnector chip would be used as the lead frame portion of a package or be monolithically integrated onto the face of the device chip itself. If the device chip was not composed of glass, release in HF solution could be performed after flip-chip assembly (rather than before), to prevent damaging the microconnectors. Care must also be taken during the flip-chip assembly to limit intermetallic effects. Material degradation of a polysilicon and gold structure is known to occur at temperatures above 250°C [10]. Also, at temperatures near 250°C, the chromium adhesion layer between the gold and silicon layers may no longer act as an effective diffusion barrier. In addition to material degradation and material migration, care must also be taken to avoid intermetallic effects with/ or contamination due to solder, particularly if indium solder is used. Minimizing the device's exposure to high temperature minimizes intermetallic effects.

HEAT TREATING

High residual stress levels are desirable for the microconnector, since increased deformation will result in increased contact force thereby decreasing contact resistance. Therefore, rather than annealing devices to relieve stress, we utilized a "heat treatment" process to introduce additional stress into our microconnectors. The tip deflection of a heat-treated connector was often two or three times greater than the post-release tip deflection of an untreated beam.

One performs the heat treatment process as follows: First, devices must be released by dissolving sacrificial layers. The connector chip is then placed on a hot stage. To treat the devices, they must be heated above their "neutral temperature", the temperature at which the beams will flatten out and become parallel to the substrate. For microconnector structures on several MUMPs runs, the neutral temperature was found to be approximately 110°C. Our heat treatment temperatures were usually between 160 and 200 °C. For treatment, one needs to maintain the chip at the heat treatment temperature long enough to reach steady state temperature (in most cases less than one minute). Once heated, the chip can be "quenched" by placing it on a cold plate. Because our microconnector chips were diced to a 2 by 2 mm size, their thermal time constant was so small that simply removing the chip from the hot plate constituted sufficient quenching.

Because manufacturing processes such as wire bonding or solder reflow can occur above a component's neutral temperature, these processes can be used to simultaneously

heat treat microconnector devices. No additional steps need be introduced to heat-treated microdevices.

Work hardening of the gold is believed to be responsible for the heat treatment effect. FCC structured materials, such as gold, are known to exhibit significant capacity for work hardening [11]. Work hardening occurs when the material is driven into its plastic deformation regime. In our heat treatment process, the thermal mismatch between gold and silicon is thought to induce work hardening.

The quantitative effects of heat treatment have already been investigated. Beam deflection was measured using a ZYGO interferometric microscope. The effects of heat treatment on a large device are much more noticeable than on a smaller device, Figure 5. Stress induced deformation of a cantilever beam varies in proportion to the square of the cantilever's length. This is in accordance with Equation 1, [5]. In the model, the tip deflection of a bimorph beam varies with the square of its length and changes linearly according to temperature. Deformation of a heat-treated beam also varies in proportion to the square of the beam's length, Figure 5. The effects of heat treatment are found to diminish over time, Figure 6. Creep based relaxation is believed to relieve some of the additional residual stress introduced into the beams during heat treatment. After 4000 hours, the tip deflection decreased by 16% of the value of the post heat treat deflection. Not all of the added residual stress is relieved, and the heat treatment does provide a long lasting enhancement of beam deflection. Experimental observation indicates that 100% improvement in tip deflection can be realized for an extended period of time.

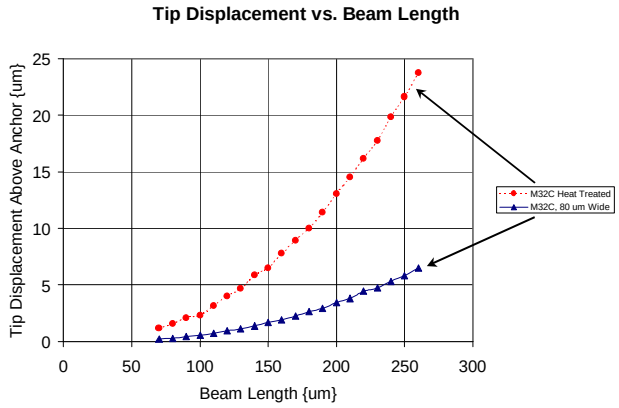

Figure 5: Tip Displacement vs. Beam Length for Heat Treated and Untreated Devices. All Beams are 80 µm Wide.

$$d = \frac{3B_1B_2E_1E_2t_1t_2(t_1+t_2)(a_2-a_1)\Delta TL^2}{(E_1B_1t_1^2)^2+(E_2B_2t_2^2)^2+2B_1B_2E_1E_2t_1t_2(2t_1^2+3t_1t_2+2t_2^2)} \quad (1)$$

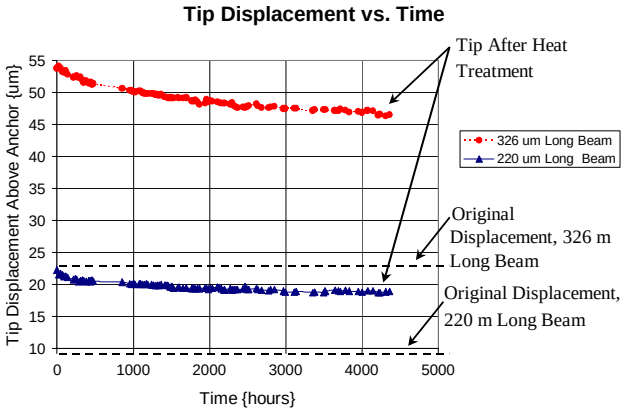

Figure 6: Relaxation of Heat Treated Bimorph Beams. The Untreated Tip Displacement Appears for Reference.

DEVICE ACTUATION BEHAVIOR

Signal switching may be achieved by actuating the cantilever beam towards the address (drive) electrode. Similar to other electrostatic devices, the microconnector is characterized by an unstable operating curve. A freestanding beam will gradually descend to the substrate as actuation potential is increased. Past a certain point, the beam will snap down to the electrode. The unstable snap-down behavior is due to non-linear nature of the electrostatic force.

The motion of a packaged microconnector is restrained during connected and disconnected states. When not being pulled down to the substrate, a microconnector will come into contact with the device chip above it. In this state, the connector presses against the device chip, establishing electrical contact, as desired. Because the device chip is in the way, the connector will not realize freestanding (unpackaged) elevation. When actuated, our devices are physically prevented from contacting the electrode by mechanical standoffs. The standoffs prevent stiction, which would otherwise occur between the beam and electrode. The physical range of motion for a microconnector is indicated in Figure 7.

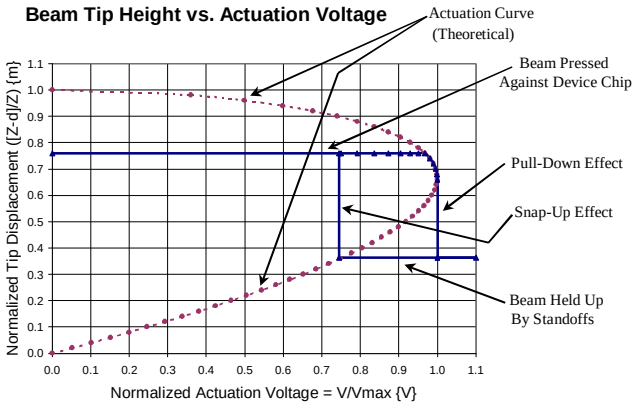

Figure 7: Actuation Profile of a Microconnector.

The actuation behavior profile may be modeled using Equations (2-6). In all equations, E refers to Young's modulus {N/m^2}, B the beam width {m}, L the beam or electrode length {m}, t the beam thickness {m}, ε the electrical permeativity {8.8419•10^{-12} {F/m} (air)}, Z_o the unactuated tip elevation {m}, δ the tip displacement from the unactuated position {m}, V the electrical potential between the beam and electrode {V}, α the thermal coefficient of expansion {1/K}, and T the temperature {K}. Subscripts '1' and '2' refer to the gold and polysilicon layers respectively, and the subscript 'e' refers to the electrode, Figure 8.

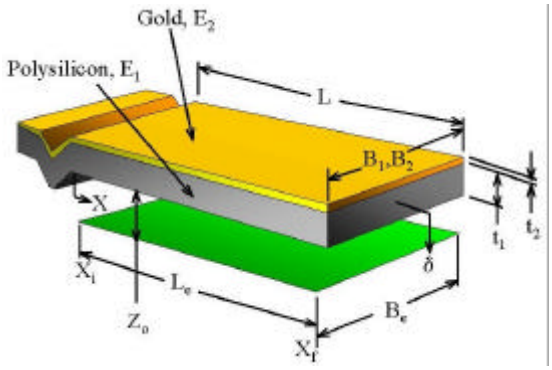

Figure 8: Variables Used in Mathematical Modeling.

$$K_{equiv} = \frac{3(EI_{equiv})}{L^3} = \left(\frac{3}{L^3}\right)\left[\frac{t_1^3 t_2 B_2 E_1 E_2}{12(E_1 t_1 + E_2 t_2)}(k)\right] \quad (2)$$

$$k = \left[4 + 6\frac{t_2}{t_1} + 4\left(\frac{t_2}{t_1}\right)^2 + \frac{E_2}{E_1}\left(\frac{t_2}{t_1}\right)^3 + \frac{E_1 t_1}{E_2 t_2}\right] \quad (3)$$

$$F_{spg} = K_{equiv}\, d \quad (4)$$

$$F_{sep} = 0.67 F_c \quad (5)$$

$$V_{pd} = (Z_o - a\, d)\sqrt{\frac{2\, b\,[(F_{spg} + F_{sep}]}{e_r e_o B_e L_e}}$$

$$\left(d = \frac{Z_o}{3a}\right) \qquad \text{when } V = V_{pd} \quad (6)$$

The designer must account for the three forces acting on a connector in contact with the device chip: the internal restoring (spring), contact separation, and electrostatic forces. The internal spring force is the result of the beam's natural tendency to return to its natural (deflected) position. Spring force is linearly proportional to the equivalent spring constant, K_{equiv} (Equations 2-4) [12], times the tip displacement. Equation 2 is valid for a cantilever (fixed-end) beam. In electrical contacts, separation force occurs due to the tendency of the contacts to adhere together. Separation force is proportional to the contact force, Equation 5 [13]. Hosaka et. al. [14] report an adhesion coefficient of 0.20 rather than 0.67. The adhesion coefficient is likely to be dependent on the process used to manufacture the contact layers. Separation force should only be considered when evaluating the pull-down voltage of a packaged device. The contact force may be estimated using Equation 4. The elevation difference between the beam's tip when it is freestanding and later assembled provides an estimate of the contact force. Finite element analysis might also be used to estimate contact force. A cantilever microconnector may generate tens or hundreds of μN of contact force depending on the design. Electrostatic force occurs when there is an electrical potential between the electrode and beam. When all forces are in equilibrium, one obtains Equation 6. Two coefficients, α and β, may be used to match the actuation profile curve to empirical results. Equation 6 [4] is based on an electrostatically actuated parallel plate. The connectors, which exhibit curved deformation, will no longer act in an ideal manner. The coefficients are a simple method of mathematically compensating for nonuniformities in behavior that occur because of the beam geometry. The coefficients are obtained at the beam's pull-down voltage.

DEVICE PERFORMANCE

The mechanical and electrical performance of a microconnector has been investigated. Common device sizes ranged from 50 to 110 μm in width and 300 to 418 μm in length. The foundry process dictates that the polysilicon and gold thickness are nominally 1.5 and 0.52 μm. Etch holes ensure proper device release. Dimples are placed midway between the etch holes and serve as standoffs during actuation.

Pull-down voltage for 418 μm long devices ranged between 53 and 66 volts, depending on beam width. The pull-down voltage is the potential required to disconnect the connector. At some point below the pull-down voltage, the connector will spring upwards, reconnecting to the device chip. The snap-up (hysteresis) voltage ranged between 43 and 61 volts. The difference between pull-down and snap-up voltages was often between 5 and 10 volts. Because of the narrow gap between pull-down and snap-up voltages, the connectors could be driven using CMOS electronics. CMOS control is possible as long as the necessary DC offset is present.

Mechanical response time was measured using an oscilloscope. The reconnect time was found to range from 5.8 to 15.2 μs, depending on beam width. Some contact bounce was observed to occur during the reconnection. Disconnect time was found to range from 4.0 to 8.5 μs. The disconnect time is the amount of time elapsed between the actuation (disconnect) signal and the onset of device discharge. That is, once disconnected, the charge retained in the formerly active device will discharge. The microconnector exhibits a first order capacitive discharge lasting approximately 34 μs.

Squeeze film damping, contact sticking, and the capacitive time constant are all thought to influence speed of

actuation. Both the connection and disconnection transition times lasted the longest when actuating wide beams. Squeeze film damping is thought to be responsible for this effect. More air must be displaced when a wider beam is used. Additional time is spent displacing the additional air underneath a wide beam. Because the connector is bounded on both sides, damping will occur during both reconnect and disconnect transitions. Sticking of contacts may influence the disconnect time. The beam must overcome surface energy forces and break cold welds in order to disconnect. The charging of the address electrode also consumes time during the disconnection. The capacitive discharge following disconnection was considerably longer than the disconnect time. The capacitive discharge is thought to be dominated by the pulldown resistor used to limit the current through the microconnectors when they were being tested.

The electrical resistance through the connector was also investigated. Connector resistance, excluding the leads and solder used to test the devices, was found to be as low as 0.89 Ω. Connector resistance values ranging between 1 and 3 Ω were common. For gold to gold microcontacts, it is theoretically possible to realize resistance values in terms of milliohms [14-16].

MAXIMUM DEVICE OPERATING CONDITIONS

During the dielectric breakdown of air, high current electrical arcs can result in catastrophic destruction. The minimum voltage required for electrical breakdown across a gap is determined by the Paschen curve. The minimum breakdown voltage in air at atmospheric pressure exists when a 327 volt potential is directed across a 7.5 μm gap [17]. Under normal operating conditions, dielectric breakdown is not expected to occur.

Another figure of interest is the device's maximum operating current. A 210 μm wide beam passed 285.3 mA of current before burning out. A 50 μm wide device conducted 235.6 mA of current before burning out. Maximum power was 1.47 and 0.76 W, respectively.

Switching the maximum current is probably not realizable. The connectors were found to fuse to the device chip before burning out. A safe, switchable current might be between 0 and 50 mA. The fusing of the connectors to the device chip is thought to be caused by contact welding. As current increases, Joule heating softens the contact surfaces, promoting contact welding. Self-heating would not only increase the likelihood of the connector fusing into place, but also affect the resistance as the throughput current increased. Resistance does vary with current, Figure 9. The current through the connector varies with the potential across the device, reflecting changes in device resistance and power dissipation, Figure 10.

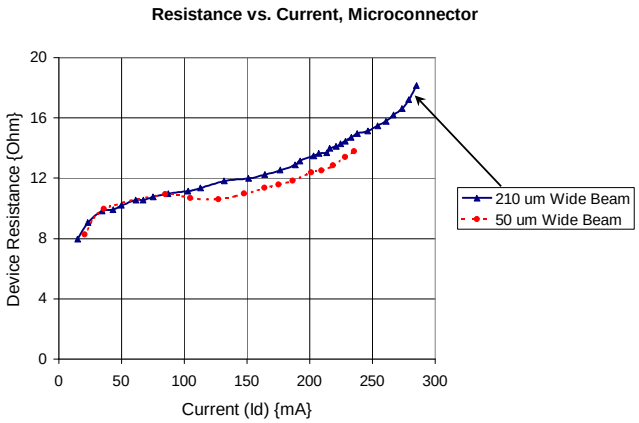

Figure 9: Resistance Through a Microconnector Varies with Current.

Device resistance is expected to increase during operation, since the increase in temperature should cause the bimorph connectors to flatten out towards the substrate. If the temperature were increased sufficiently, the beams might disconnect from the device chip above. Rather than disconnecting, the tips of the failed devices were observed to weld to the contact pads on the device chip. The extent of contact welding appears to have been so great that the connectors could not disconnect.

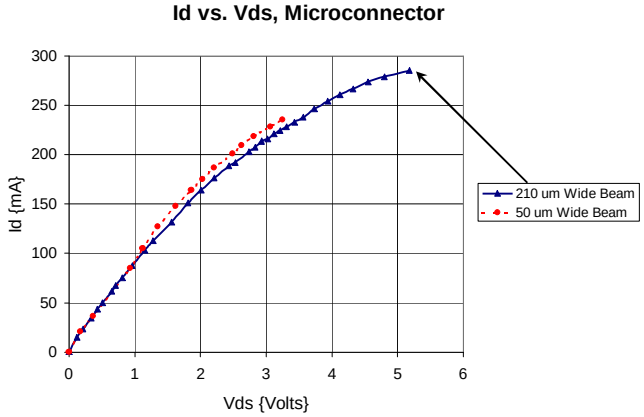

Figure 10: Microconnector I/V Profile.

Examination of failed devices demonstrates the need for connectors to be designed to promote both electrical and thermal conduction. Apparently, the beams vaporized in their midsection when heat could not be sufficiently dissipated, Figure 11. Conduction is the dominant heat transfer mechanism in almost all microdevices. It is not surprising that the portion of the beam furthest from contact with other surfaces (which serve as heat sinks) would burn out first. At its mid-length, the beam, which serves as the path of heat flux, is furthest from both microconnector and device chips, the two heat sinks.

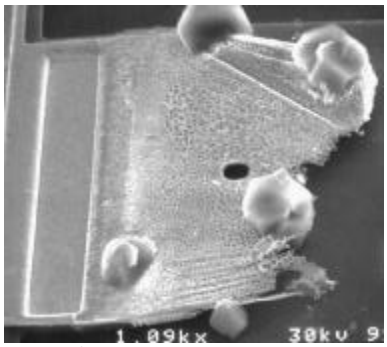

Figure 11: Anchor of Connector Destroyed During the Maximum Current Characterization.

Examining the I/V characteristics reveals that the current and voltage capacity of the connectors are near required levels. A 3.5 volt potential is sufficient for applications involving current generations of computer microprocessors. Greater power dissipation and lower device resistance are expected to be realizable, if one uses thicker material layers. This would ensure a factor of safety in design. Note that device capacity data, including Figures 9 & 10, pertain to the total device, including leads and solder joints. Device resistance values, mentioned in the previous section and Table 1, represent the true resistance of the connectors themselves, and exclude the resistance of leads, and solder joints. Lead resistance was found to be roughly equivalent to the true device resistance.

Table 1: Summary of Connector Performance.

Device Parameters	Minimum (Typical)	Maximum (Typical)
Length {um}	300	418
Width {um}	50	110
Freestanding Deflection at Tip {um}	16.98	61.87
Contact Resistance {Ohm}	0.89	3.17
Pull Down Voltage {V}	53	66
Snap Up (Hysteresis) Voltage {um}	43	61
Disconnect Time {us}	4	8.5
Reconnect Time {us}	5.8	15.2
Maximum Current {mA}	235.6	285.3
Maximum Power {W}	0.76	1.47

Looking back at device performance reveals that the connector's width holds influence over several performance parameters, Table 1. Narrow beams were found to actuate more rapidly than wide beams. Wide beams were found to have a lower pull-down voltage, higher current carrying capability, and higher power dissipation capability. A design compromise exists between operating speed and almost all other performance parameters.

CONCLUSION

An actuatable microconnector for use in electronics packaging has been demonstrated. The connectors are meant to be flip-chip assembled underneath so-called device chips. Heat treatment can be used to increase the deformation of the bimorph beams. The affects of heat treatment become more significant as beam length increases and are long lasting in nature. The operating behavior of our connectors is similar to many other electrostatically operated microdevices and may be mathematically modeled in a similar manner. Narrow connector beams operate fastest, while wide beams require lower actuation potential, have higher current carrying capability and power dissipation ability. Connectors were observed to burn out in their midsection, the portion of the beam, located in the gap between the microconnector and device chips. Burnout behavior illustrates the need to design for both electrical and thermal conductivity.

REFERENCES

[1] K. Petersen, "Dynamic Micromechanics on Silicon: Techniques and Devices", IEEE Transactions on Electron Devices, 25(10), October 1978, pp. 1241-1250.

[2] J. Yao, and F. Chang, "A Surface Micromachined Miniature Switch for Telecommunications Applications with Signal Frequencies From DC up to 4 GHz", Proceedings Solid-State Sensors and Actuators (Transducers '95), June 25-29, 1995, pp. 384-387.

[3] I. Schiele, and B. Hillerich, "Comparison of Lateral and Vertical Switches for Application as Microrelays", Journal of Micromechanics and Microengineering, (9), 1999, pp. 146-150.

[4] P. Zavracky, S. Majumder, and N. McGruer, "Micromechanical Switches Fabricated Using Nickel Surface Micromachining", Journal of Microelectromechanical Systems, 6(1), 1997, pp. 3-9.

[5] Y. Zhang, Y. Zhang and R. Marcus, "Thermally Actuated Microprobes for a New Wafer Probe Card", Journal of Microelectromechanical Systems, 8(1), 1999, pp. 43-49.

[6] Y. Yi, Y. Kondoh, K. Ihara, and M. Saitoh, "A Micro Active Probe Device Compatible with SOI-CMOS Technologies", Journal of Microelectromechanical Systems, 6(3), 1997, pp. 242-248.

[7] K. Markus, and D. Koester, "Multi-User MEMS Process (MUMPS) Introduction & Design Rules", 3021 Cornwallis Road, Research Triangle Park, North Carolina: MCNC Electronics Tech. Div, June 1998.

[8] G. Mulhern, S. Soane, and R. Howe, "Supercritical Carbon Dioxide Drying for Microstructures", IEEE Solid-State Sensor and Actuator Workshop, Hilton Head, SC, USA, 1996, pp. 42-47.

[9] W. Lin, S. Patra, and Y.C. Lee, "Design of Solder Joints for Self-Aligned Opto-Electronic Assemblies", IEEE Trans. Components, Packaging and Manufacturing, August 1995, pp. 543-551.

[10] D. Burns, and V. Bright, "Investigation of the Maximum Optical Power Rating for a Micro-Electro-Mechanical Device", 1997 International Conference on Solid-State Sensors and Actuators (Transducers-97), 1997, pp. 335-338.

[11] H. Frost and M. Ashby, *Deformation Mechanism Maps: The Plasticity and Creep of Metals and Ceramics*, New York: Pergamo Press, 1982.

[12] W. Young, *Roark's Formulas for Stress & Strain*, New York: McGraw-Hill, 1975, pp. 112-115.

[13] R. Curthell, and D. Tipping, "Electric Contacts. II: Mechanics of Closure for Gold Contacts." Journal of Applied Physics, 44(1), 1973, pp. 4360-4365

[14] H. Hosaka, H. Kuwano, and K. Yanagisawa, "Electromagnetic Microrelays: Concepts and Fundamental Characteristics", IEEE Micro Electro Mechanical Systems (MEMS '93), 1993, pp. 12-17.

[15] J. Schimkat, "Contact Materials for Microrelays", IEEE Micro Electro Mechanical Systems (MEMS '98), 1998, pp. 190-194.

[16] D. Hyman, and M. Mehregany, "Contact Physics of Gold Microcontacts for MEMS Switches", Proc. 44th IEEE Holm Conference on Electrical Contacts, 1998, pp. 133-140.

[17] Bell Telephone Laboratories Incorporated, *Physical Design of Electronic Systems Volume III: Integrated Device and Connection Technology*, Prentice-Hall: Englewood Cliffs, 1971, pp. 439-654.